A Metalens Array on a 12-inch Glass Wafer for Optical Dot Projection

Ting Hu*, Qize Zhong, Nanxi Li, Yuan Dong, Zhengji Xu, Dongdong Li, Yuan Hsing Fu, Yanyan Zhou, Keng Heng Lai, Vladimir Bliznetsov, Hou-Jang Lee, Wei Loong Loh, Shiyang Zhu, Qunying Lin and Navab Singh

Institute of Microelectronics, Agency for Science Technology and Research, 2 Fusionopolis Way, #08-02, Innovis, Singapore 138634
**Corresponding author: hut@ime.a-star.edu.sg*

Abstract: We report the first demonstration of a metalens array fabricated on a 12-inch glass wafer for dot projection. Good uniformity in dot size is achieved, with a maximum deviation of 8% to the simulated value.
OCIS codes: (220.0220) Optical design and fabrication; (110.5220) Photolithography; (310.6628) Subwavelength structures, nanostructures.

1. Introduction

Metasurface provides an alternative scheme to implement optical components with various functionalities in a miniaturized size [1]. In these metasurface-based optical components, metalenses have attract a lot of research interests due to their wide applications [2-4]. Since the basic function of a metalens is to focus the incoming light beam to a spot at the focal plane, the metalens array can be used to generate a cloud of optical dots, which is useful for three-dimensional (3D) sensing, facial recognition and motion detection [5–7]. The consumer electronics demand the large-scale, cost-effective and mass-producible dot projector. However, for metasurface patterning, the electron beam lithography (EBL) is commonly used [3,4], it requires long processing time and hence cannot meet the demand for mass production.

In this paper, we report the demonstration a metalens array on a 12-inch glass wafer working at 940 nm for dot projection. The metalens is designed using the 3D finite-difference time-domain (FDTD) method together with the ray tracing method, and then fabricated in house by a 12-inch complementary metal-oxide-semiconductor (CMOS)-compatible fabrication line [8-11]. The metalens array is characterized in an imaging system. The optical dots are observed by the beam profiler. The performance of the metalens agrees well with the simulation.

2. Device Design, Fabrication and Characterization

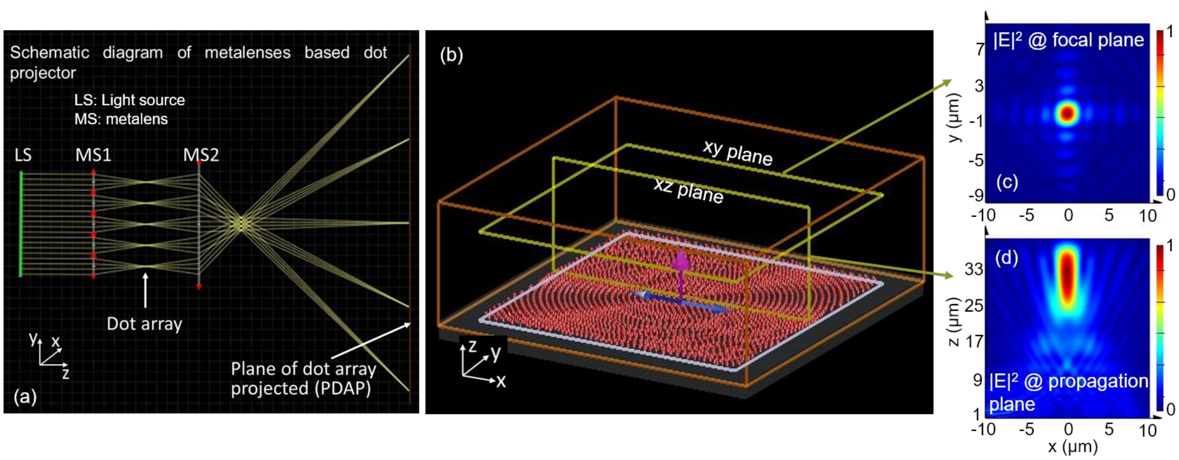

Fig. 1 (a) The schematic diagram of the proposed optical dot projector, (b) the configuration of the metalens as a building block in the array, the simulated E intensity of the metalens at the (c) focal and (d) propagation plane.

The schematic diagram of the proposed dot projector is show in Fig. 1(a). The dot projector is composed by two layers of metasurfaces. The 1st layer metasurface is the metalens array, which focus the incoming light beam into the dot array on the focal plane, while the 2nd one is a whole metalens to project the dot array to a plane with a designed distance. The schematic configuration of the metalens in the array is shown in Fig. 1(b). It is built by engineering the spatial distribution of the nano cylindrical a-Si pillars on the glass substrate to meet a parabolic phase profile [11]. The 3D-FDTD simulation results of the 20 μm-diameter metalens are shown in Fig. 1(c) and 1(d). One can see that the light beam is focused into a spot at a distance of 31.8 μm from the metalens surface, with a spot size of around 1.7 μm. The spacing between two adjacent optical dots (focal spots) is 20 μm. In order to project the dots to a certain distance with larger spacing, a 2nd metalens is needed. The magnification of the dot spacing, can be expressed as

$$\mathrm{A}=\frac{w}{h}=\frac{f+d}{f+a}\approx\frac{d}{f},(\mathrm{a}\ll\mathrm{f},\mathrm{f}\ll\mathrm{d}) \tag{1}$$

Where f is the focal length, a+f is the object distance, d+f is projected plane distance, h is the original spacing between two dots, and w is the dot spacing at the projected plane. All the parameters are marked in Fig. 2(a). To save the calculating time, a 3 × 3 metalens array is simulated for concept proof. The simulated E intensity profile at the 3 × 3 metalens array surface is shown in Fig. 2(b). After a propagating distance of the focal length, the 3 × 3 optical dots are formed at the focal plane (~31.8 μm from the metalen array surface) with a spacing of 20 μm, as shown Fig. 2(b). By a design of A=100, after the propagation through the 2nd metalens, the spacing between the dots is enlarged to 2 mm as shown in Fig. 2(d), which is 100 times magnification of the original spacing. In this dot projection system, the metalens array is the key component, thus we will focus on the demonstration of it in the rest part.

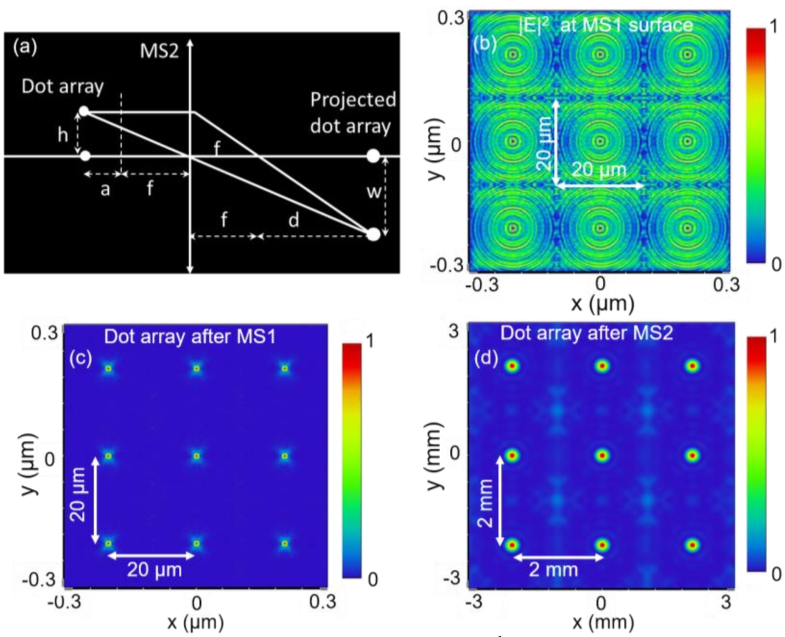

Fig. 2 (a) The schematic diagram of the beam propagation through the 2nd metalens, the simulated E intensity profile at (b) the surface and (c) the focal plane of the metalens array, (d) the simulated E intensity profile with 100 times magnification of dot spacing after the 2nd metalens.

The metalens array is fabricated using the CMOS-compatible fabrication facilities. A 400 nm thick a-Si is deposited using the plasma-enhanced chemical vapor deposition (PECVD) on a 12-inch glass substrate. Two opaque thin film layers are used at the bottom and the top of the wafer to overcome the wafer non-detectable issue in the fabrication machine and the focusing of the UV light during the photolithography process, respectively. The 193 nm ArF DUV and inductively coupled plasma (ICP) etch were used to make the a-Si pillars of the metalens.

The photograph of the fabricated a-Si metalens array on a 12-inch glass wafer is shown in Fig. 3 (a). The metalens array in one of the repeated dies is located at where the white arrow points. The characterization setup is the same with that used in [11]. Fig. 3(b) and 3(c) are the scanning electron microscope (SEM) pictures showing part of the metalens array and the building block metalens, respectively. The E intensity profile at the metalens array surface and focal plane are shown in Fig. 3(d) and 3(e). It can be observed clearly that the dot array is captured by the beam profiler. The E intensity at the propagation plane of the x cut is shown in Fig. 3(f). The measured focal length is around 32 μm, which is quite close to the designed 31.8 μm (NA=0.3). The optical intensity of the x cut is plotted in Fig. 3(g), from which the extracted spot/dot size (the width at half maximum) is ranging from 1.6 μm to 1.86 μm, which is close to the numerically simulated dot size of 1.74 μm. The dot size deviation may attribute to the imperfect a-Si pillar dimensions and random defects induced in the fabrication process. It will be improved by optimizing the fabrication process.

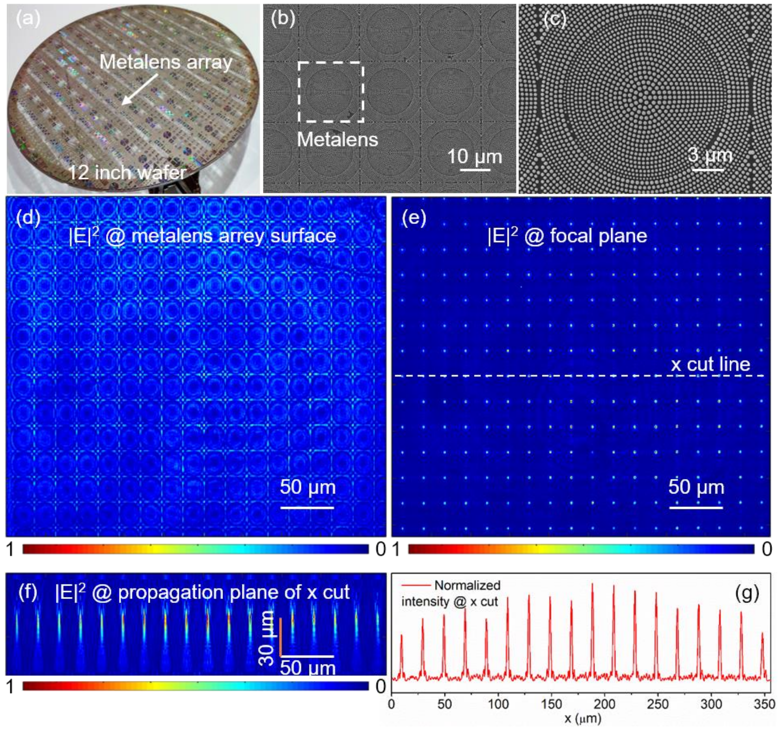

Fig. 3 (a) The photograph of the fabricated a-Si metalens array on a 12-inch glass wafer, the SEM pictures of (b) the metalens array and (c) the building block metalens, the measured E intensity at the (d) metalens surface, (e) focal plane, and (f) propagation plane, (g) the normalized optical intensity of the dots on the x cut line. Limited to the size of the opto-electronic sensor, 13 × 18 dots are observed rather than the designed 25 × 25.

3. Conclusion

In summary, a 25 × 25 metalens array working at 940 nm for dot projection is realized on a 12-inch glass wafer using CMOS-compatible technology. The measurement results agree well with the design. The demonstrated mass-producible dot projector with a miniature size has potential applications in the compact consumer electronics for 3D sensing, facial recognition and motion detection.

The authors acknowledge the RIE2020 Advanced Manufacturing and Engineering (AME) Domain's Core Funds: SERC Strategic Funds (A1818g0028)

4. References

1. N. Yu and F. Capasso, “Flat optics with designer metasurfaces,” Nat. Mat. 13, pp. 139-150, (2014).
2. M. Khorasaninejad and F. Capasso, “Metalenses: Versatile multifunctional photonic components,” Science 358(6367), eaam8100, (2017).
3. W. T. Chen, A. Y. Zhu, V. Sanjeev, M. Khorasaninejad, Z. Shi, E, Lee, and F. Capasso, “A broadband achromatic metalens for focusing and imaging in the visible,” Nat. Nanotechnol. 13, pp. 220-226 (2018).
4. S. Wang, P C. Wu, V.-C. Su, Y.-C. Lai, M.-K. Chen, H. Y. Kuo, B. H. Chen, Y. H. Chen, T.-T. Huang, J.-H. Wang, R.-M. Lin, C.-H. Kuan, T. Li, Z. Wang, S. Zhu, and D. P. Tsai, “A broadband achromatic metalens in the visible,” Nat. Nanotechnol. 13, pp. 227-232 (2018).
5. Z. Li, Q. Dai, M. Q. Mehmood, G. Hu, B. L. yanchuk, J. Tao, C. Hao, I. Kim, H. Jeong, G. Zheng, S. Yu, A. Alù, J. Rho, and C.-W. Qiu, "Full-space Cloud of Random Points with a Scrambling Metasurface," Light: Science & Applications 7(1), 63 (2018).
6. M. Morinaga, X. Gu, K. Shimura, M. Nakahama, A. Matsutani, and F. Koyama, "VCSEL Amplifier Dot Projector with Folded-Path Slow-Light Waveguide for 3D Depth Sensing," in 2018 IEEE International Semiconductor Laser Conference (ISLC) (2018), pp. 1–2.
7. K. Hisatomi, M. Kano, K. Ikeya, M. Katayama, T. Mishina, Y. Iwadate, and K. Aizawa, "Depth Estimation Using an Infrared Dot Projector and an Infrared Color Stereo Camera," IEEE Transactions on Circuits and Systems for Video Technology 27(10), 2086–2097 (2017).
8. Z. Xu, Y. Dong, C.-K. Tseng, T. Hu, J. Tong, Q. Zhong, N. Li, L. Sim, K. H. Lai, Y. Lin, D. Li, Y. Li, V. Bliznetsov, Y.-H. Fu, S. Zhu, Q. Lin, D. H. Zhang, Y. Gu, N. Singh, and D.-L. Kwong, "CMOS-compatible all-Si metasurface polarizing bandpass filters on 12-inch wafers," Opt. Express 27(18), 26060–26069 (2019).
9. N. Li, H. Y. Fu, Y. Dong, T. Hu, Z. Xu, Q. Zhong, D. Li, K. H. Lai, S. Zhu, Q. Lin, Y. Gu, and N. Singh, "Large-area pixelated metasurface beam deflector on a 12-inch glass wafer for random point generation," Nanoph 8(10), 1855 (2019).
10. Z. Xu, Y. Dong, Y. H. Fu, Q. Zhong, T. Hu, D. Li, Y. Li, N. Li, Y. Lin, Q. Lin, S. Zhu, and N. Singh, "Embedded dielectric metasurface based subtractive color filter on a 300mm glass wafer," in Conference on Lasers and Electro-Optics, OSA Technical Digest (Optical Society of America, 2019), p. STh1O.4.
11. T. Hu, Q. Zhong, N. Li, Y. Dong, Y. Hsing Fu, Z. Xu, D. Li, V. Bliznetsov, K. H. Lai, S. Zhu, Q. Lin, Y. Gu, N. Singh, and D.-L. Kwong, "Demonstration of a-Si metalenses on a 12-inch glass wafer by CMOS-compatible technology," arXiv e-prints arXiv:1906.11764 (2019).